HD-THEP-08-31, FTUAM 08/22, IFT-UAM/CSIC-08-83

Large non-Gaussianity from two-component hybrid inflation

Christian T. Byrnes*
Institut für Theoretische Physik, Universität Heidelberg, Philosophenweg 16, 69120 Heidelberg, Germany

Ki-Young Choi†
Departamento de Física Teórica C-XI, Universidad Autónoma de Madrid, Cantoblanco, 28049 Madrid, Spain and Instituto de Física Teórica UAM/CSIC, Universidad Autónoma de Madrid, Cantoblanco, 28049 Madrid, Spain

Lisa M.H. Hall‡
Department of Applied Mathematics, University of Sheffield, Sheffield, S3 7RH, UK
(Dated: February 12, 2009)

We study the generation of non-Gaussianity in models of hybrid inflation with two inflaton fields, (2–brid inflation). We analyse the region in the parameter and the initial condition space where a large non-Gaussianity may be generated during slow-roll inflation which is generally characterised by a large $f_{\rm NL}$, τ_{NL} and a small g_{NL}. For certain parameter values we can satisfy $\tau_{NL} \gg f_{\rm NL}^2$. The bispectrum is of the local type but may have a significant scale dependence. We show that the loop corrections to the power spectrum and bispectrum are suppressed during inflation, if one assume that the fields follow a classical background trajectory. We also include the effect of the waterfall field, which can lead to a significant change in the observables after the waterfall field is destabilised, depending on the couplings between the waterfall and inflaton fields.

PACS numbers: 98.80.Cq

I. INTRODUCTION

The increasingly accurate observations of the cosmic microwave background [1] motivate the study of inflation beyond linear order in perturbation theory. Since there are many models of inflation which give similar predictions for the spectral index of the scalar perturbations and the tensor-to-scalar ratio [2, 3] it is important to consider higher order observables. Non-Gaussianity has emerged as a powerful discriminant between different models of inflation. Any detection of primordial non-Gaussianity would rule out the simplest models of single field inflation.

Many ways to generate a large non-Gaussianity have been proposed in the literature [4, 5, 6, 7, 8, 9]. If the inflaton has a non-canonical kinetic term then the inflaton field perturbations may already be non-Gaussian at Hubble exit during inflation [10]. Otherwise the perturbations are Gaussian at Hubble exit and any non-Gaussianity must then be generated on super Hubble scales [11, 12]. Popular methods to generate a large non-Gaussianity after inflation include having a feature in the inflaton potential [13], the curvaton scenario [14], modulated reheating/preheating [15, 16], an inhomogeneous end of inflation [17, 18, 19, 20, 21] or by loop domination of the bispectrum or trispectrum [22, 23]. Work has also been done on calculating the non-Gaussianity during inflation with a separable potential [24, 25, 26, 27] and with more general potentials [28, 29]. Recently the authors of this paper have shown that it is possible to generate a large non-Gaussianity during multiple field inflation while keeping all of the slow-roll parameters much less than unity [30].

In this paper we study this possibility of generating a large non-Gaussianity during slow-roll inflation in detail for the specific model of hybrid inflation. We consider carefully the parameter constraints and initial conditions required to do this. Unlike in the previous work [30] we here also consider the effect of the waterfall field required to end inflation. We can therefore also compare and contrast our work to a recent paper on generating a large non-Gaussianity at the end of inflation [21]. Depending on the values of the couplings between the two inflaton fields and the waterfall field observable quantities may change when the waterfall field is destabilised. This change in the primordial curvature perturbation is possible because there are isocurvature perturbations present at the end of inflation.

*Electronic address: C.Byrnes@thphys.uni-heidelberg.de
†Electronic address: kiyoung.choi@uam.es
‡Electronic address: lisa.hall@sheffield.ac.uk

We also calculate further observables for this model, such as the trispectrum and the scale dependence of the bispectrum. In most cases the trispectrum is large through a large τ_{NL} whenever the bispectrum is large but the relation between them also depends on the initial conditions.

Recently it has also been shown that for two-field hybrid inflation it is possible to generate a large loop correction to the bispectrum and trispectrum [22, 23]. For a special trajectory it was shown that the bispectrum can be observably large even when the tree level value of the bispectrum is slow-roll suppressed. Here we show that this is not possible for a classical trajectory, since we require that the classical motion of the field dominates over its quantum fluctuations in order that a slow-roll calculation is valid.

The plan of our paper is as follows: In Section II we review the generation of a large bispectrum during hybrid inflation and calculate the trispectrum. In Section III we include the waterfall field and consider its effect at the end of inflation for different couplings between the waterfall and inflaton fields and further evolution after inflation. In Section IV we calculate the scale dependence of the non-Gaussianity parameter. We conclude in Section V. In the Appendix, we show that the loop correction is subdominant to the tree level term for the power spectrum, bispectrum and trispectrum.

II. NON-GAUSSIANITY DURING HYBRID INFLATION

We consider a model of two field hybrid inflation, whose potential is given by

$$W(\varphi,\chi) = W_0\left(1+\frac{1}{2}\eta_{\varphi\varphi}\frac{\varphi^2}{M_P^2}+\frac{1}{2}\eta_{\chi\chi}\frac{\chi^2}{M_P^2}\right), \tag{1}$$

which is vacuum dominated, i.e. which satisfies $\left|\eta_{\varphi\varphi}\varphi^2\right| \ll M_P^2$ and $\left|\eta_{\chi\chi}\chi^2\right| \ll M_P^2$. We assume that inflation ends abruptly by a waterfall field which is heavy during inflation and hence doesn't affect the dynamics during inflation. In this section we calculate observables during slow-roll inflation. We will consider the full potential including the waterfall field in Sec. III. We will see that this can lead to a change in observables on the surface where the waterfall field is destabilised.

In the vacuum dominated regime the slow-roll solutions are

$$\varphi = \varphi_* e^{-\eta_{\varphi\varphi}N}, \qquad \chi = \chi_* e^{-\eta_{\chi\chi}N}, \tag{2}$$

where '*' denotes the value at the horizon exit. Throughout this section whenever we write a quantity without making it explicit at which time it should be evaluated, we mean the equation to be valid at any time N e–foldings after Hubble exit and while slow roll is valid. Generally we will be interested in quantities at the end of inflation, in which case we take $N = 60$.

The slow-roll parameters are

$$\epsilon_\varphi = \frac{1}{2}\eta_{\varphi\varphi}^2\frac{\varphi^2}{M_P^2}, \qquad \epsilon_\chi = \frac{1}{2}\eta_{\chi\chi}^2\frac{\chi^2}{M_P^2}, \qquad \epsilon = \epsilon_\varphi + \epsilon_\chi. \tag{3}$$

We note that the dominant slow-roll parameters $\eta_{\varphi\varphi}$ and $\eta_{\chi\chi}$ are constants during inflation in the vacuum dominated regime and that they are much larger than the slow-roll parameters ϵ_φ and ϵ_χ throughout inflation.

Using the δN formalism [31, 32, 33, 34, 35] (for details see the appendix) we can calculate the power spectrum $\mathcal{P}_\zeta$, spectral index n_ζ, tensor-to scalar ratio r, where $\mathcal{P}_T$ is the power spectrum of tensor perturbations, and the non-linearity parameter $f_{\rm NL}$ in this model [5, 24, 25, 30, 36], at leading order,

$$\mathcal{P}_\zeta = \frac{W_*}{24\pi^2 M_P^4\epsilon^2}\left(\epsilon_\varphi e^{-2\eta_{\varphi\varphi}N}+\epsilon_\chi e^{-2\eta_{\chi\chi}N}\right), \tag{4}$$

$$\begin{aligned} n_\zeta - 1 &= -2\epsilon^* + 2\frac{(\eta_{\varphi\varphi}-2\epsilon e^{2\eta_{\varphi\varphi}N})\epsilon_\varphi e^{-2\eta_{\varphi\varphi}N}+(\eta_{\chi\chi}-2\epsilon e^{2\eta_{\chi\chi}N})\epsilon_\chi e^{-2\eta_{\chi\chi}N}}{\epsilon_\varphi e^{-2\eta_{\varphi\varphi}N}+\epsilon_\chi e^{-2\eta_{\chi\chi}N}} \\ &\simeq 2\frac{\eta_{\varphi\varphi}\epsilon_\varphi e^{-2\eta_{\varphi\varphi}N}+\eta_{\chi\chi}\epsilon_\chi e^{-2\eta_{\chi\chi}N}}{\epsilon_\varphi e^{-2\eta_{\varphi\varphi}N}+\epsilon_\chi e^{-2\eta_{\chi\chi}N}}, \end{aligned} \tag{5}$$

$$r \equiv \frac{\mathcal{P}_T}{\mathcal{P}_\zeta} = \frac{16\epsilon^2}{\epsilon_\varphi e^{-2\eta_{\varphi\varphi}N} + \epsilon_\chi e^{-2\eta_{\chi\chi}N}}, \tag{6}$$

$$f_{\rm NL} = \frac{5}{6}\frac{-\epsilon\left[\eta_{\varphi\varphi}\epsilon_\varphi + \eta_{\chi\chi}\epsilon_\chi e^{4(\eta_{\varphi\varphi}-\eta_{\chi\chi})N}\right] + \frac{2}{\epsilon}\epsilon_\varphi\epsilon_\chi(\eta_{\varphi\varphi}\epsilon_\chi + \eta_{\chi\chi}\epsilon_\varphi)\left[1 - e^{2(\eta_{\varphi\varphi}-\eta_{\chi\chi})N}\right]^2}{\left[\epsilon_\varphi + \epsilon_\chi e^{2(\eta_{\varphi\varphi}-\eta_{\chi\chi})N}\right]^2}. \tag{7}$$

According to [30], large non-Gaussianity can be realised in either of two regions

$$\cos^2\theta \equiv \frac{\dot\varphi^2}{\dot\varphi^2 + \dot\chi^2} \simeq \frac{\epsilon_\varphi}{\epsilon_\varphi + \epsilon_\chi} \ll 1, \qquad \text{or} \qquad \sin^2\theta \equiv \frac{\dot\chi^2}{\dot\varphi^2 + \dot\chi^2} \simeq \frac{\epsilon_\chi}{\epsilon_\varphi + \epsilon_\chi} \ll 1. \tag{8}$$

Since both regions are symmetrical [30] (before specifying the values of $\eta_{\varphi\varphi}$ and $\eta_{\chi\chi}$), in the rest of this paper we will focus on the second region (Region B or D in Ref. [30]). In this region where $\epsilon_\varphi \gg \epsilon_\chi$, $|f_{\rm NL}| > 1$ is fulfilled by the condition,

$$\sin^2\theta^* \lesssim \sin^4\theta\left(\sqrt{\frac{5|\eta_{\chi\chi}|}{6\sin^2\theta}} - 1\right), \tag{9}$$

in other words,

$$|\eta_{\chi\chi}|^{-1} e^{-4(\eta_{\varphi\varphi}-\eta_{\chi\chi})N} \lesssim \sin^2\theta \simeq \frac{\epsilon_\chi}{\epsilon_\varphi} \lesssim |\eta_{\chi\chi}|. \tag{10}$$

This condition implies three conditions on the parameter θ:

$$\sin^2\theta^* < \frac{1}{3}\left(\frac{5}{6}\right)^2\left(\frac{3}{4}\right)^4|\eta_{\chi\chi}|^2, \quad \sin^2\theta < \frac{5}{6}|\eta_{\chi\chi}|, \qquad \frac{\sin^2\theta}{\sin^2\theta^*} > \frac{24}{5}\frac{1}{|\eta_{\chi\chi}|}. \tag{11}$$

Note that in this region $\sin\theta \simeq \eta_{\chi\chi}\chi/(\eta_{\varphi\varphi}\varphi)$, from Eq. (2) we require $N(\eta_{\varphi\varphi} - \eta_{\chi\chi}) > 1$ so that $\sin^2\theta$ grows significantly during inflation.

A. Simplified formula for the observables when $f_{\rm NL}$ is large

We can substantially simplify all of the above formula in the case where $f_{\rm NL}$ is large. We define the quantity

$$\tilde r \equiv \left(\frac{\partial N}{\partial\chi_*}\right)^2 / \left(\frac{\partial N}{\partial\varphi_*}\right)^2 = \frac{\epsilon_\chi}{\epsilon_\varphi} e^{2(\eta_{\varphi\varphi}-\eta_{\chi\chi})N}. \tag{12}$$

In the region we are considering where $f_{\rm NL}$ is large, this is approximately given by the initial and final angles of the background trajectory with different exponents

$$\tilde r \simeq \frac{\sin^4\theta}{\sin^2\theta^*}. \tag{13}$$

We note that $\tilde r$ can be either larger or smaller than one.

In the case of large non-Gaussianity it follows that

$$\mathcal{P}_\zeta \simeq \frac{W_*}{24\pi^2 M_P^4 \epsilon_*}\left(1 + \frac{\epsilon_\chi}{\epsilon_\varphi} e^{2(\eta_{\varphi\varphi}-\eta_{\chi\chi})N}\right) = \frac{8}{r}\left(\frac{H_*}{2\pi}\right)^2, \tag{14}$$

$$n_\zeta - 1 \simeq 2\frac{\eta_{\varphi\varphi} + \tilde r\eta_{\chi\chi}}{1 + \tilde r}, \tag{15}$$

$$r \simeq \frac{16\epsilon^*}{1+\tilde{r}}, \tag{16}$$

$$f_{\rm NL} \simeq \frac{5}{6}\frac{\sin^6\theta^e}{(\sin^2\theta^* + \sin^4\theta^e)^2}\eta_{\chi\chi} = \frac{5}{6}\frac{\tilde{r}}{(1+\tilde{r})^2}\eta_{\chi\chi}e^{2(\eta_{\varphi\varphi}-\eta_{\chi\chi})N}. \tag{17}$$

The first condition in Eq. (11) implies that

$$\frac{\chi_*}{\varphi_*} \ll 1. \tag{18}$$

We therefore require a very small value of χ_* in order to have a large non-Gaussianity. We will see in sec II B that there is a limit to how small we can make χ_* while χ still follows a classical slow-roll trajectory. In practise for relatively large values of $\eta_{\varphi\varphi} - \eta_{\chi\chi}$ this places a bound on how large we can make $f_{\rm NL}$.

The sign of $f_{\rm NL}$ is determined by the sign of $\eta_{\chi\chi}$. The amplitude of $f_{\rm NL}$ depends exponentially on the difference of the slow-roll parameters, $\eta_{\varphi\varphi}-\eta_{\chi\chi}$, which we require to be positive to be in the branch of large non-Gaussianity where $\sin^2\theta \ll 1$. However the spectral index depends on the weighted sum of the slow-roll parameters, so it is possible to have a large non-Gaussianity and a scale invariant spectrum. However it is not possible to have a large and positive $f_{\rm NL}$ and a red spectrum of perturbations. We will see in Sec. III B that by including the effect of the waterfall field this conclusion may change, depending on the values of the coupling constants between the two inflaton fields and the waterfall field.

Using the δN formalism we can also calculate the non-linearity parameters which parameterise the trispectrum. There are two shape independent parameters, which may be observationally distinguishable and are given by [37]

$$f_{\rm NL} = \frac{5}{6}\frac{N_{AB}N_AN_B}{(N_CN_C)^2}, \qquad \tau_{NL} = \frac{N_{AB}N_{BC}N_AN_C}{(N_DN_D)^3}, \qquad g_{NL} = \frac{25}{54}\frac{N_{ABC}N_AN_BN_C}{(N_DN_D)^3}, \tag{19}$$

where summation over the fields is implied over the repeated indices A, B, C, D. For comparison we also give the formula for $f_{\rm NL}$ [35]. In the regime where $|g_{NL}| > 1$ it is given by

$$g_{NL} = \frac{10}{3}\frac{\tilde{r}\,(\eta_{\varphi\varphi} - 2\eta_{\chi\chi}) - \eta_{\chi\chi}}{1+\tilde{r}}f_{\rm NL}. \tag{20}$$

Details of the calculation for both g_{NL} and τ_{NL} are in the appendix, in particular see Eqs. (51), (52) and (67). We see that g_{NL} is subdominant to $f_{\rm NL}$ and hence won't provide a competitive observational signature. The current observational bound on the local type of the bispectrum from WMAP data is $-9 < f_{\rm NL} < 111$ at the 2σ level [1] and currently there is no observational constraint on the trispectrum. If there is no detection it is expected that with Planck data the bounds will be reduced to about $|f_{\rm NL}| \lesssim 10$ and $\tau_{NL} \lesssim 560$ [38].

However in the regime where τ_{NL} is large, which is similar to the region where $f_{\rm NL}$ is large we find

$$\tau_{NL} = \frac{\tilde{r}}{(1+\tilde{r})^3}\eta_{\chi\chi}^2 e^{4N(\eta_{\varphi\varphi}-\eta_{\chi\chi})} = \frac{1+\tilde{r}}{\tilde{r}}\left(\frac{6}{5}f_{\rm NL}\right)^2. \tag{21}$$

From Eq. (17) we see that for given model parameters $\eta_{\varphi\varphi}$ and $\eta_{\chi\chi}$ the value of $f_{\rm NL}$ is maximised for $\tilde{r} = 1$, i.e. when we choose the initial field values to satisfy

$$\frac{\chi_*}{\varphi_*} = \frac{\eta_{\varphi\varphi}}{\eta_{\chi\chi}}e^{-2N(\eta_{\varphi\varphi}-\eta_{\chi\chi})}. \tag{22}$$

In this case the non-linearity parameters are given by

$$f_{\rm NL} = \frac{5}{24}\eta_{\chi\chi}e^{2N(\eta_{\varphi\varphi}-\eta_{\chi\chi})}, \qquad \tau_{NL} = 2\left(\frac{6}{5}f_{\rm NL}\right)^2. \tag{23}$$

However τ_{NL} is maximised at a slightly different point, for $\tilde{r} = 1/2$.

It follows from (21) that $\tau_{NL} > (6f_{\rm NL}/5)^2$, so τ_{NL} may be large and provide an extra observable parameter for this model. This inequality between τ_{NL} and $f_{\rm NL}$ is true in general [16], and equality is reached whenever a single field direction during inflation generates the primordial curvature perturbation. However it is usually assumed that $\tau_{NL} \sim f_{\rm NL}^2$ since both arise from second derivatives in the δN formalism. In fact for our model it is possible to have

$\eta_{\varphi\varphi}$	$\eta_{\chi\chi}$	φ_*	χ_*	φ_e	χ_e	$\tilde{r}$	$f_{\rm NL}$	τ_{NL}	g_{NL}	$n_\zeta - 1$	r
0.04	-0.04	1	6.8×10^{-5}	0.091	7.50×10^{-5}	1	-123	4.4×10^4	-33	0	0.006
0.04	-0.04	1	1.5×10^{-4}	0.091	1.65×10^{-3}	5	-68	8×10^3	-24	-0.05	0.002
0.08	0.01	1	0.0018	0.008	9.88×10^{-4}	1	9.27	247	0.77	0.09	0.026
0.02	-0.04	1	0.00037	0.301	4.08×10^{-3}	1	-11.1	357	-2.6	-0.02	0.002
-0.01	-0.09	1	3×10^{-6}	1.822	6.64×10^{-4}	0.16	-132	1.8×10^5	-44	-0.04	0.0007
0.06	-0.01	1	4.3×10^{-4}	0.027	7.84×10^{-4}	0.1	-3	148	-0.2	0.11	0.026
0.01	-0.06	1	7.5×10^{-6}	0.549	2.75×10^{-4}	0.04	-8	2.5×10^3	-2	0.01	0.0008

TABLE I: Table showing some initial conditions for the hybrid inflation model that lead to large levels of non-Gaussianity. The end point of fields, $\tilde{r}$, the bispectrum and trispectrum non-linearity parameters, spectral index and tensor-to-scalar ratio are shown. They are evaluated when the number of e-foldings from the end of inflation is $N_k = 60$.

a small $f_{\rm NL}$ (and hence also a small g_{NL}) but a large and potentially observable τ_{NL}. For this we require that $\tilde{r} \ll 1$, in practice if we make it too small it may no longer be possible to satisfy the classical constraint (24) discussed in Sec. II B. In the final example in Table I we give an explicit example of parameter values which give rise to an $f_{\rm NL}$ which is probably too small to be detected with Planck but with a very large trispectrum through $\tau_{NL} > 10^3$ that should be detectable at a high significance. For another example with $f_{NL}, g_{NL} \lesssim O(1)$ but $\tau_{NL} \gg 1$, see [39]. In contrast it has been shown in several papers [37, 40, 41, 42, 43] that in the curvaton scenario where the curvaton has a non-quadratic potential it is possible to realise $|g_{NL}| \gg 1$ while $\tau_{NL} = (6f_{\rm NL}/5)^2$ is small with some tuning of parameters. Recently it has also been shown that in a single field model with a non-canonical kinetic term it is possible for certain tuned parameters to achieve a much larger trispectrum than bispectrum [44]. We note that the non-Gaussianity in their model has a very different shape dependence to the k independent non-linearity parameters we are considering in this paper.

In Table I, we give some explicit examples of values of $\eta_{\varphi\varphi}$, $\eta_{\chi\chi}$, φ_* and χ_* which lead to a large non-Gaussianity. Using Eq. (5) we also calculate the spectral index. The contours of $f_{\rm NL}$ of potential for a specific choice of $\eta_{\varphi\varphi}$ and $\eta_{\chi\chi}$ is given in Fig.5 in our previous paper [30]. We correct tensor-to-scalar ratio in Table 1 of [30]. [1] The first example in the Table I shows that it is possible to have $|f_{\rm NL}| \simeq 100$ and a scale invariant spectrum. We also see that it is possible to generate a large non-Gaussianity during slow roll with $\eta_{\varphi\varphi}$ and $\eta_{\chi\chi}$ both positive or both negative, or when one is positive and the other negative corresponding to a saddle point.

B. Can the loop correction dominate?

Cogollo *et al.* have calculated the effect of the loop correction to the primordial power spectrum and bispectrum [22] and even more recently Rodriguez and Valenzuela-Toledo have calculated the loop correction to the trispectrum [23]. In both cases this was for the special case of a straight background trajectory where one of the fields is zero throughout inflation. This loop correction arises from taking into account the contribution to the power spectrum and bispectrum arising from terms in the δN expansion which are non-leading in the expansion of the field perturbation $\delta\varphi_*$, see e.g. [45]. However they can still be significant if the coefficient to the term given by the second derivative of N with respect to the subdominant field is extremely large and the leading term for the same field is small or zero, e.g. [46]. These "higher order" terms are usually neglected, but [22] has shown the first explicit example of an inflation model where they cannot be neglected. They consider a 2-field hybrid model with the same potential as Eq. (1) in the special case of an unstable straight trajectory along one of the axes, with $\eta_{\varphi\varphi}$ and $\eta_{\chi\chi}$ both negative. In this case, they find (for certain initial values) that one of the loop correction terms is dominant over the tree level term and can generate an observable $f_{\rm NL}$.

However if the value becomes too small then the motion of the χ field will become dominated by quantum fluctuations rather than the classical drift down the potential, $3H\dot{\chi} \simeq -W_\chi = -W_0\eta_{\chi\chi}\chi/M_P^2$, which we have assumed. In order that we can neglect the effect of the quantum fluctuations, the condition we require on the background trajectory is [47]

$$|\dot{\chi}|\pi/H^2 > \sqrt{3/2}. \tag{24}$$

[1] The value of the tensor-to-scalar ratio in Table 1 of [30] is incorrect. The correct value for the first row is 0.005, for the second row is 0.026 (as given in Table I) and for the third row $r = 0.002$. This does not change the discussion or conclusions of [30].

We require the condition above to be satisfied throughout inflation. Since the fields in our model either increase or decrease monotonically it is sufficient to check that the constraint is satisfied both at Hubble exit and at the end of inflation. In the appendix we show that satisfying this condition requires that the loop corrections are suppressed. We have checked that for the examples in Table I this condition is satisfied. We stress that this suppression of the loop corrections follows from the requirement that the background trajectory of the inflation fields is dominated by the classical motion. However it would be interesting to investigate the large loop corrections found in [22, 23] using a calculation which includes the quantum corrections to the χ field, which is set to zero throughout inflation in [22, 23].

Because we have shown that the loop correction is always suppressed compared to the tree level terms we are justified in using the formula for the tree-level non-Gaussianity parameters as given by Eq. (19).

III. NON-GAUSSIANITY AFTER HYBRID INFLATION

In this section we include the effects of the waterfall field ρ which is required to end hybrid inflation. Inflation ends when the waterfall field is destabilised, i.e. when its effective mass becomes negative. During inflation the waterfall field is heavy and it is trapped with a vacuum expectation value of zero, so we can neglect it during inflation. The end of inflation occurs when the effective mass of the waterfall field is zero, which occurs on a hypersurface defined in general by [20, 21],

$$\sigma^2 = G(\varphi, \chi) \equiv g_1^2\varphi^2 + g_2^2\chi^2, \tag{25}$$

which is realised by the potential $W(\varphi, \chi)$, defined by Eq. (1), where W_0 is given by

$$W_0 = \frac{1}{2}G(\varphi, \chi)\rho^2 + \frac{\lambda}{4}\left(\rho^2 - \frac{\sigma^2}{\lambda}\right)^2. \tag{26}$$

Here g_1 (g_2) is the coupling between the φ (χ) field and the waterfall field. In general the hypersurface defined by this end condition is not a surface of uniform energy density. Because the δN formalism requires one to integrate up to a surface of uniform energy density we need to add a small correction term to the amount of expansion up to the surface where the waterfall field is destabilised, which we will consider in sec. III C.

We note here that the hybrid potential, which we have written in the form of a sum potential can also be written as a product potential in the limit of vacuum domination. We show this so that we can use the formula from [21], we consider a potential of the form

$$W(\varphi, \chi) = W_0 \exp\left(\frac{1}{2}\eta_{\varphi\varphi}\frac{\varphi^2}{M_P^2}\right)\exp\left(\frac{1}{2}\eta_{\chi\chi}\frac{\chi^2}{M_P^2}\right). \tag{27}$$

We note that the slow-roll parameters are not exactly the same from these two ways of writing the potential, but that we are only interested in calculating results at leading order in slow roll, and in this limit the two ways of writing the hybrid potential are equivalent.

This is an example of a model with an inhomogeneous end of inflation, i.e. where inflation ends at slightly different times in different places. This has been studied as a method for converting the inflationary isocurvature perturbation into the primordial curvature perturbation [18]. It has also been shown for the hybrid potential we are considering that this can be used to generate a large amount of non-Gaussianity, for certain parameters values and fine tuning of the parameters [19, 21]. However these papers concern the large non-Gaussianity generated at the end of inflation rather than during slow-roll inflation, by having a very large ratio of couplings $g_1/g_2 \ll 1$. Here we consider the case where g_1 and g_2 have the same order of magnitude with $g_1^2/g_2^2 = \eta_{\varphi\varphi}/\eta_{\chi\chi}$ in sec. III A and with $g_1^2 = g_2^2$ in sec. III B.

A. $g_1^2/g_2^2 = \eta_{\varphi\varphi}/\eta_{\chi\chi}$

In this case we have chosen the coupling constants (which can satisfy $g_1^2 < 0$ and/or $g_2^2 < 0$) such that the surface where the waterfall field is destabilised corresponds to a surface of uniform energy density. In this case the value of all observable quantities such as the power spectrum and non-Gaussianity are the same as those we calculated previously which were valid at the final hypersurface of uniform energy density during inflation.

With these values of the coupling constants, large non-Gaussianity can only be generated with the special conditions we have outlined earlier in this paper and it is given by Eq. (14) – Eq. (17). We have checked that our result for $f_{\rm NL}$, Eq. (7) in this case is consistent with the formula for $f_{\rm NL}$ in [21]. This provides a check on the algebra. We

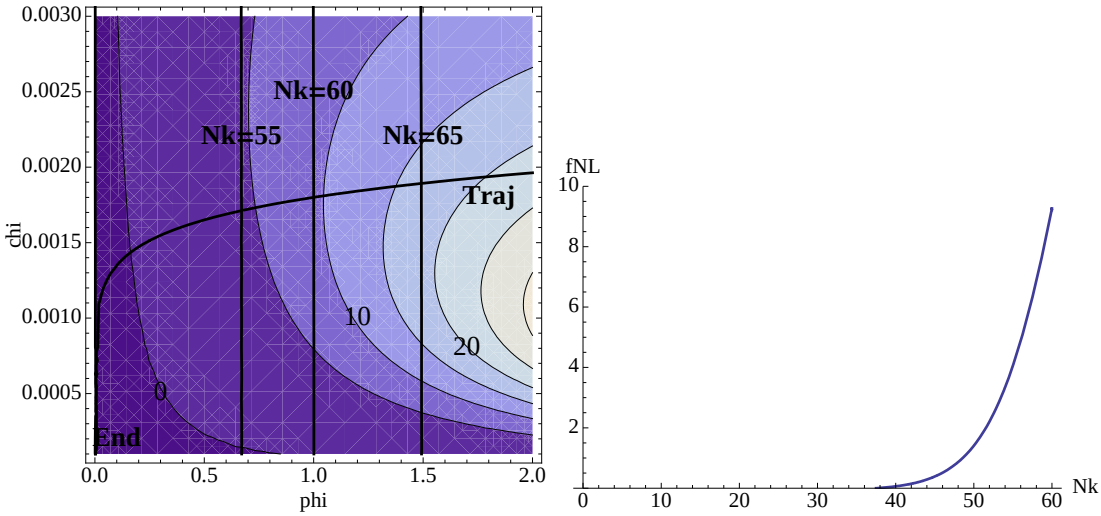

FIG. 1: Left: The contour plot of $f_{\rm NL}$ which have the end condition same as uniform energy density hypersurface $g_1^2/g_2^2 = \eta_{\varphi\varphi}/\eta_{\chi\chi}$ in III A in the plane of phi and chi, which denote the values of the fields when the given scale leaves the horizon. The values of $f_{\rm NL}$, 0, 10 and 20, are shown on the corresponding contour. For example with the given end point, the trajectory is shown as a line denoted by "Traj". The cross point with $N_k = 60$ line is the value of phi and chi when the scale corresponding to $N_k = 60$ leaves horizon. In this scale the value of $f_{\rm NL}$ is around 9. Right: Directly from the left figure, we can read the scale dependence of $f_{\rm NL}$ on the given trajectory. For the given trajectory the spectrum of $f_{\rm NL}$ is shown in the figure. For this trajectory we used the third example in Table I, i.e. $\eta_{\varphi\varphi} = 0.08$, $\eta_{\chi\chi} = 0.01$, and the end point is fixed so that the field values $\varphi_* = 1$ and $\chi_* = 0.0018$ lead to the number of e-foldings $N_k = 60$.

emphasise that this large non-Gaussianity is not from the end of inflation but from the evolution during inflation. To compare between our paper and [21] we note that in their notation $m_1^2 = \eta_{\varphi\varphi}$, $m_2^2 = \eta_{\chi\chi}$, $\epsilon_\varphi^e = -m_1^3 m_2 \varphi_e \chi_e W/(2Z)$ and $\epsilon_\chi^e = m_1 m_3^3 \varphi_e \chi_e Y/(2X)$ where the parameters W, X, Y and Z are defined in [21].

In the left hand plot of figure 1, we show the contour plot of $f_{\rm NL}$ in the (φ, χ) plane of the field values when the given scale leaves the horizon. $f_{\rm NL}$ increase as the number of e-folding from the end of inflation increases, which is shown in the right figure. This can be easily understood from Eq. (17). For a small e-folding number, N_k, (corresponding to small scales) $\tilde{r}$ is also small and $f_{\rm NL}$ is small. As N_k increases, $\tilde{r}$ increases as well as $f_{\rm NL}$. However for $\tilde{r} \gtrsim 1$, which corresponds to $N_k \gtrsim [\log(\epsilon_\varphi/\epsilon_\chi)]/2(\eta_{\varphi\varphi} - \eta_{\chi\chi})$ for a given end point, $f_{\rm NL}$ approaches its the maximum value, which corresponds to

$$f_{\rm NL}^{max} = \frac{5}{6}\frac{\epsilon_\varphi}{\epsilon_\chi}\eta_{\chi\chi}. \tag{28}$$

In the example given in Fig. 1, this happens around $N_k \gtrsim 120$, thus the maximum is not shown in the right-hand plot of Fig. 1 in the given range of N_k. The value of N_k which gives the maximum value can be modified by the condition of end of inflation and can be approached $N_k \sim 60$ which is shown in the next section and Fig. 2.

B. $g_1^2 = g_2^2$

In this case, the end of inflation given by the condition in Eq. (25) does not occur on a uniform energy density hypersurface [21]. In this subsection we will show how the non-Gaussianity is modified by the condition at the end of inflation with this specific example. In general we expect there to be some modification to non-Gaussianity from the end of inflation, except in the special case we considered in III A.

In this case the power spectrum and the non-linearity parameters are [21]

$$\mathcal{P}_\zeta \simeq \frac{W_0}{24\pi^2 M_P^4}\frac{(\epsilon_\varphi/\eta_{\varphi\varphi}^2)e^{-2\eta_{\varphi\varphi}N} + (\epsilon_\chi/\eta_{\chi\chi}^2)e^{-2\eta_{\chi\chi}N}}{(\epsilon_\varphi/\eta_{\varphi\varphi} + \epsilon_\chi/\eta_{\chi\chi})^2}, \tag{29}$$

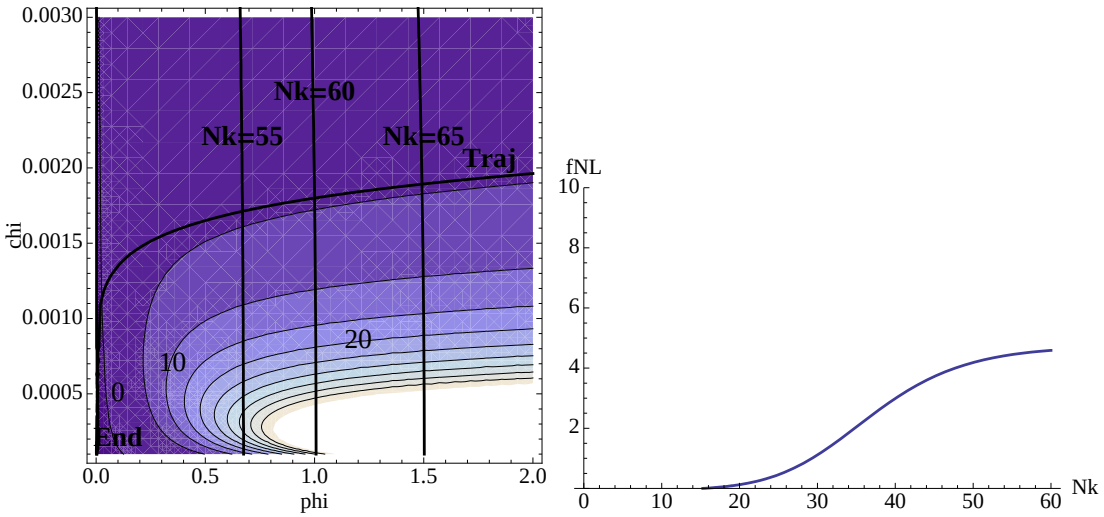

FIG. 2: Same as Fig. 1 but using the end condition $g_1^2 = g_2^2$, see III B.

$$f_{\rm NL} = \frac{5}{6}\frac{-\left(\epsilon_\varphi/\eta_{\varphi\varphi}^2 + \epsilon_\chi/\eta_{\chi\chi}^2 e^{4(\eta_{\varphi\varphi}-\eta_{\chi\chi})N}\right)\left(\epsilon_\varphi/\eta_{\varphi\varphi} + \epsilon_\chi/\eta_{\chi\chi}\right) + 2\frac{\epsilon_\varphi\epsilon_\chi}{\eta_{\varphi\varphi}^2\eta_{\chi\chi}^2}\frac{\epsilon_\varphi/\eta_{\varphi\varphi}^2+\epsilon_\chi/\eta_{\chi\chi}^2}{\epsilon_\varphi/\eta_{\varphi\varphi}+\epsilon_\chi/\eta_{\chi\chi}}(\eta_{\chi\chi} - \eta_{\varphi\varphi}e^{2(\eta_{\varphi\varphi}-\eta_{\chi\chi})N})^2}{\left[\epsilon_\varphi/\eta_{\varphi\varphi}^2 + \epsilon_\chi/\eta_{\chi\chi}^2 e^{2(\eta_{\varphi\varphi}-\eta_{\chi\chi})N}\right]^2}. \tag{30}$$

In the large $f_{\rm NL}$ limit,

$$\mathcal{P}_\zeta \simeq \frac{W_*}{24\pi^2 M_P^4 \epsilon_*}\left(1 + \frac{\eta_{\varphi\varphi}^2}{\eta_{\chi\chi}^2}\frac{\epsilon_\chi}{\epsilon_\varphi}e^{2(\eta_{\varphi\varphi}-\eta_{\chi\chi})N}\right) = \frac{8}{r}\left(\frac{H_*}{2\pi}\right)^2, \tag{31}$$

$$n_\zeta - 1 \simeq 2\frac{\eta_{\varphi\varphi} + \frac{\eta_{\varphi\varphi}^2}{\eta_{\chi\chi}^2}\tilde{r}\eta_{\chi\chi}}{1 + \frac{\eta_{\varphi\varphi}^2}{\eta_{\chi\chi}^2}\tilde{r}}, \tag{32}$$

$$r \simeq 16\epsilon^*\left(1 + \frac{\eta_{\varphi\varphi}^2}{\eta_{\chi\chi}^2}\tilde{r}\right)^{-1}, \tag{33}$$

$$f_{\rm NL} \simeq \frac{5}{6}\frac{\frac{\eta_{\varphi\varphi}^2}{\eta_{\chi\chi}^2}\tilde{r}}{\left(1 + \frac{\eta_{\varphi\varphi}^2}{\eta_{\chi\chi}^2}\tilde{r}\right)^2}\eta_{\varphi\varphi}e^{2(\eta_{\varphi\varphi}-\eta_{\chi\chi})N}. \tag{34}$$

We can see that the observables at the end of inflation are changed by the additional ratio of $\eta_{\varphi\varphi}^2/\eta_{\chi\chi}^2$ before $\tilde{r}$. Furthermore, $f_{\rm NL}$ has an additional factor of $\eta_{\varphi\varphi}/\eta_{\chi\chi}$.

In Table II we show the values of $f_{\rm NL}$, $n_\zeta - 1$ and r for the same parameter values as we used in Table I. The first two examples show that if $\eta_{\varphi\varphi} = -\eta_{\chi\chi}$ then the observables are unchanged except that the sign of $f_{\rm NL}$ is switched. The second example in the table shows that in this case it is possible to have a red spectral index and a positive value of $f_{\rm NL}$. For many values of the initial parameters when $|\eta_{\varphi\varphi}/\eta_{\chi\chi}| \neq 1$ the magnitude of $f_{\rm NL}$ decreases compared to Table I. We see that this is the case for most examples given in the table. This is most strikingly illustrated in the fifth example in the two tables. We can see by comparing (17) and (34) that in the case where $\tilde{r} \ll 1$ and $|\eta_{\varphi\varphi}/\eta_{\chi\chi}| \ll 1$ that the magnitude of $f_{\rm NL}$ will decrease by about $|\eta_{\varphi\varphi}/\eta_{\chi\chi}|^3$. However for most values of $\tilde{r}$ and the ratio $\eta_{\varphi\varphi}/\eta_{\chi\chi}$ the change is much smaller. In some cases $f_{\rm NL}$ increases, by the largest amount when $\tilde{r} < 1$ and $|\eta_{\varphi\varphi}/\eta_{\chi\chi}| > 1$. An example of this where $|f_{\rm NL}|$ grows by more than an order of magnitude is shown in the sixth column of Tables I and

$\eta_{\varphi\varphi}$	$\eta_{\chi\chi}$	φ_*	χ_*	$\tilde{r}$	$f_{\rm NL}$	$n_\zeta - 1$	r
0.04	-0.04	1	6.8×10^{-5}	1	123	0	0.006
0.04	-0.04	1	1.5×10^{-4}	5	68	-0.05	0.002
0.08	0.01	1	0.0018	1	4.59	0.02	0.0008
0.02	-0.04	1	0.00037	1	3.5	0.02	0.026
-0.01	-0.09	1	3×10^{-6}	0.16	-0.2	-0.02	0.0008
0.06	-0.01	1	4.3×10^{-4}	0.1	38	0.01	0.006

TABLE II: Same as Table I but with different end condition, $g_1^2 = g_2^2$ as used in sec. III B.

II.

Due to the additional factor before $\tilde{r}$, $f_{\rm NL}$ is increased at small scales compared to the case in sec. III A and decreased at large scales due to the additional factor. Thus the maximum $f_{\rm NL}$ is smaller than that of sec. III A by $\eta_{\varphi\varphi}/\eta_{\chi\chi}$. At small scales (where $\tilde{r} \ll 1$), $f_{{\rm NL}\,A} = (\eta_{\varphi\varphi}/\eta_{\chi\chi}) f_{{\rm NL}\,B}$. At large scales (where $\tilde{r} \gg 1$), $f_{{\rm NL}\,A} = (\eta_{\chi\chi}/\eta_{\varphi\varphi}) f_{{\rm NL}\,B}$.

C. The end of hybrid inflation

As we mentioned in the previous sections, the end of inflation given by the condition in Eq. (25) does not occur on a uniform energy density hypersurface [21], i.e. the energy density is slightly different for the different end points. For the δN formalism to be valid, δN should be calculated at the uniform energy density hypersurface. This is explained in [20] with the extra term N_c in Eq. (3.14) of [20]. They assume that the universe has become radiation-dominated right after inflation. This means that at the time t_e when the water fall field starts to become unstable, the energy density of the inflaton fields changes to radiation instantly conserving the energy density, ignoring the details of the water fall field dynamics. If we define the time t_c sometime in the radiation dominated era, the change in the number of e–foldings between t_e and t_c is

$$N_c = \frac{1}{4} \ln \left[\frac{W_f}{W_0} \right]. \tag{35}$$

This can be understood like this: During radiation domination, [48]

$$\frac{d\rho}{dN} = -4\rho, \tag{36}$$

which gives

$$N_c = N(t_c) - N(t_e) = \frac{1}{4} \ln \frac{\rho_e}{\rho_c} = \frac{1}{4} \ln \frac{W_f}{W_c} = \frac{1}{4} \ln \frac{W_f}{W_0} + \frac{1}{4} \ln \frac{W_0}{W_c}. \tag{37}$$

where we can put $W_c = W_0$ which anyway does not change δN. This is Eq. (3.15) in [20]. We require that the perturbation from this term, δN_c, is smaller than from δN_f. This was shown for the hybrid potential with a linear exponential dependence on the field in [20], but it was not shown in [21] where they consider the same hybrid potential as we do, with a quadratic dependence on the fields. Therefore we need to check the validity of neglecting δN_c in our two examples in the previous subsections.

In the first example with $g_2^2/g_1^2 = \eta_{\varphi\varphi}/\eta_{\chi\chi}$, as in sec. III A, the hypersurface at the end of inflation is a uniform energy density hypersurface, which means $\delta N_c = 0$. Thus in this case, there is no further change of f_{NL}, if we assume an instantaneous change to radiation.

In the other case with $g_1^2 = g_2^2$, as in sec. III B, we obtain

$$N_c = \frac{1}{4} \ln \frac{W_f}{W_0} = \frac{1}{8} \left(\eta_{\varphi\varphi} \varphi^2 + \eta_{\chi\chi} \chi^2 \right). \tag{38}$$

Taking the perturbation of N_c, we find

$$\delta N_c = \frac{\sigma^2}{8 g_1^2} (\eta_{\chi\chi} - \eta_{\varphi\varphi}) \left[(\sin 2\gamma)(\delta_1\gamma + \delta_2\gamma) + (\cos 2\gamma)(\delta_1\gamma)^2 \right], \tag{39}$$

where γ is defined by $\tan\gamma = \chi/\varphi$ at the end of inflation satisfying Eq. (25). Using the expressions for $\delta_1\gamma$ and $\delta_2\gamma$

((Eq (A2) and (A4) respectively in [21]), this becomes

$$\delta N_c = \frac{\sigma^2}{8g_1^2}(\eta_{\chi\chi}-\eta_{\varphi\varphi})\left[\sin 2\gamma \frac{-\eta_{\chi\chi}\frac{\delta\varphi_*}{\varphi_*}+\eta_{\varphi\varphi}\frac{\delta\chi_*}{\chi_*}}{\eta_{\chi\chi}\tan\gamma+\eta_{\varphi\varphi}/\tan\gamma}+\frac{\sin 2\gamma}{2}\frac{\eta_{\chi\chi}\left(\frac{\delta\varphi_*}{\varphi_*}\right)^2-\eta_{\varphi\varphi}\left(\frac{\delta\chi_*}{\chi_*}\right)^2}{\eta_{\chi\chi}\tan\gamma+\eta_{\varphi\varphi}/\tan\gamma}\right.$$
$$\left.+\frac{1}{2}\frac{\left\{\left(-\eta_{\chi\chi}/\cos^2\gamma+\eta_{\varphi\varphi}/\sin^2\gamma\right)\sin 2\gamma+\cos 2\gamma(\eta_{\chi\chi}\tan\gamma+\eta_{\varphi\varphi}/\tan\gamma)\right\}\left(\eta_{\chi\chi}\frac{\delta\varphi_*}{\varphi_*}-\eta_{\varphi\varphi}\frac{\delta\chi_*}{\chi_*}\right)^2}{\left(\eta_{\chi\chi}\tan\gamma+\eta_{\varphi\varphi}/\tan\gamma\right)^3}\right]. \tag{40}$$

The perturbation of N from the flat hypersurface at horizon exit during inflation to the hypersurface at the end of the inflation (with a corrected factor of one half missing in (A.8) in [21]),

$$\delta N = \frac{1/\tan\gamma\frac{\delta\varphi_*}{\varphi_*}+\tan\gamma\frac{\delta\chi_*}{\chi_*}}{\eta_{\chi\chi}\tan\gamma+\eta_{\varphi\varphi}/\tan\gamma}+\frac{1}{2}\frac{-1/\tan\gamma\left(\frac{\delta\varphi_*}{\varphi_*}\right)^2+\tan\gamma\left(\frac{\delta\chi_*}{\chi_*}\right)^2}{\eta_{\chi\chi}\tan\gamma+\eta_{\varphi\varphi}/\tan\gamma}+\frac{1/(\sin\gamma\cos\gamma)\left(\eta_{\chi\chi}\frac{\delta\varphi_*}{\varphi_*}-\eta_{\varphi\varphi}\frac{\delta\chi_*}{\chi_*}\right)^2}{\left(\eta_{\chi\chi}\tan\gamma+\eta_{\varphi\varphi}/\tan\gamma\right)^3}. \tag{41}$$

The final δN_f from the flat hypersurface at horizon exit during inflation to the uniform energy density hypersurface during radiation dominated era is the sum of both

$$\delta N_f = \delta N + \delta N_c. \tag{42}$$

By comparing the corresponding term of $\delta\varphi_*/\varphi$, $\delta\chi_*/\chi$ etc between δN_c and δN, we find that the term in δN_c is suppressed compared to the corresponding term in δN by

$$\frac{\sigma^2}{8g_1^2}(\eta_{\chi\chi}-\eta_{\varphi\varphi})\times(\eta_{\varphi\varphi}\quad\text{or}\quad\eta_{\chi\chi})\times(\sin^2\gamma\quad\text{or}\quad\cos^2\gamma). \tag{43}$$

Here $\frac{\sigma^2}{g_1^2}=\varphi^2+\chi^2$. Since we are working in the vacuum dominated regime and slow-roll, Eq. (3), $\frac{\sigma^2}{g_1^2}\eta_{\varphi\varphi}^2\ll 1$ and $\frac{\sigma^2}{g_1^2}\eta_{\chi\chi}^2\ll 1$. We therefore see that δN_c is greatly suppressed compared to δN.

D. Further evolution after inflation

So far in this section we have assumed a quick transition to the radiation epoch at the end of inflation, thereby neglecting the dynamics of the waterfall field. However if we consider the role of the waterfall field, then after the waterfall field is destabilised there may be a further evolution of the primordial curvature perturbation, which will lead to a change of the observable parameters. This applies to any model with an inhomogeneous end of inflation since there are isocurvature perturbations still present after the waterfall field is destabilised and inflation has ended. Further evolution will depend on the details of reheating in a model dependent way. To the best of our knowledge this issue has not been considered in depth in any paper on an inhomogeneous end of inflation. If we assume an instantaneous transition to radiation domination (so a completely efficient and immediate decay of the waterfall and inflaton fields) then there will be no further change to the observables as we have argued in the previous section. However this is clearly an idealised case. For a review of reheating after inflation see for example [49].

In the special case where the waterfall field is also light during inflation Barnaby and Cline [7] have shown there is the possibility of generating a large non-Gaussianity during preheating for certain parameter values. This is possible even if there is only one inflaton field and the waterfall field present. However in this case inflation does not end abruptly when the waterfall field is destabilised so this is not the scenario we have considered in this paper.

In practice the efficiency of reheating will depend on the couplings between the waterfall and inflaton fields to any preheat fields, as well as on the ratio between g_1, g_2 and λ [50]. In one regime where $\lambda \gg g_1$ and g_2 preheating depends mainly on the inflaton fields. In the case where the two inflaton fields couple identically to all further particles preheating depends on the coupling constants g_1 and g_2 and only much more weakly on their bare masses proportional to $\eta_{\varphi\varphi}$ and $\eta_{\chi\chi}$ [50]. So in the case where $g_1 = g_2$ which we have considered earlier it may be reasonable to expect little or no further evolution of the curvature perturbation, because the isocurvature perturbations should be irrelevant and decay during preheating. On the other hand if $g_1/g_2 \ll 1$ which is the case considered in some previous works on an inhomogeneous end to inflation the effect from preheating is more likely to be important. In another regime where $\lambda \ll g_1$ and g_2 preheating depends mainly on the waterfall field, so it may be that in this case the isocurvature

perturbations are again unimportant. However we should also consider the period from when the waterfall field is destabilised and until preheating begins. It could be that the amount of expansion during this time also leads to an extra correction to the curvature perturbation. This is a complicated issue which deserves further investigation but is beyond the scope of this paper. To the best of our knowledge there has been no study of preheating or reheating in a model of hybrid inflation with more than one inflaton field.

IV. SCALE DEPENDENCE

In general the bispectrum parameterised by $f_{\rm NL}$ can have both a scale and a shape dependence. We are considering the local form of $f_{\rm NL}$ which means that $f_{\rm NL}$ is shape independent. However it can still have a (slow-roll suppressed) scale dependence [51, 52, 53].

In our examples $f_{\rm NL}$ has a scale dependence both because of the exponential term in $f_{\rm NL}$, (17), and because $\tilde{r}$ will vary through the change of the initial value of $\sin^2\theta^*$. We find

$$\frac{\partial \ln \tilde{r}}{\partial \ln k} = \frac{\partial \ln e^{2N(\eta_{\varphi\varphi}-\eta_{\chi\chi})}}{\partial \ln k} = -2(\eta_{\varphi\varphi}-\eta_{\chi\chi}). \tag{44}$$

Using this we find from (17) that

$$n_{f_{\rm NL}} - 1 \equiv \frac{d\log f_{\rm NL}}{d\log k} = -4\frac{\eta_{\varphi\varphi}-\eta_{\chi\chi}}{1+\tilde{r}}. \tag{45}$$

In the case that we include the effect from the surface where the waterfall field is destabilised and $g_1^2 = g_2^2$ we find from (34) that

$$n_{f_{\rm NL}} - 1 = -4\frac{\eta_{\varphi\varphi}-\eta_{\chi\chi}}{1+\left(\frac{\eta_{\varphi\varphi}}{\eta_{\chi\chi}}\right)^2\tilde{r}}. \tag{46}$$

For both cases the spectral index of $f_{\rm NL}$ satisfies

$$-4(\eta_{\varphi\varphi}-\eta_{\chi\chi}) < n_{f_{\rm NL}} - 1 < 0, \tag{47}$$

for any value of $\tilde{r}$ and hence $f_{\rm NL}$ will be smaller on small scales as we can see in the figures 1 and 2.

Because we require a relatively large value of $\eta_{\varphi\varphi}-\eta_{\chi\chi} > 1/N$ for our model to generate a large non-Gaussianity it is quite possible for our model to generate a relatively significant scale dependence of $f_{\rm NL}$. However the amount also depends on $\tilde{r}$ and when this is large then $n_{f_{\rm NL}} - 1$ is suppressed.

We note that this is in contrast to the large non-Gaussianity from an inhomogeneous end of inflation found in [21]. In the specific cases they considered to generate a large non-Gaussianity the non-Gaussianity was generated purely at the end of inflation and $f_{\rm NL}$ is scale independent. In detail we see from Eqs. (4.4) and (4.24) in [21] that their formulae for $f_{\rm NL}$ does not depend on N or on any quantities evaluated at Hubble exit.

V. CONCLUSION

We have made an in depth study of a model of hybrid inflation with two inflaton fields (two-brid inflation). We have studied the parameter space where non-Gaussianity may be large during slow-roll inflation. In particular we have calculated the observable parameters $\mathcal{P}_\zeta$, $n_\zeta - 1$, r, $f_{\rm NL}$, g_{NL} and τ_{NL}. The spectral index depends on the weighted sum of the slow-roll parameters $\eta_{\varphi\varphi}$ and $\eta_{\chi\chi}$ while the bispectrum depends exponentially on the difference of the same slow-roll parameters, so it is possible to have a very large bispectrum and a scale invariant spectrum. We have shown that the trispectrum is generally large through τ_{NL} whenever the bispectrum is large, but that the other parameter which parameterises the trispectrum, g_{NL} is always smaller than $f_{\rm NL}$ and strongly suppressed compared to τ_{NL}. We have also shown that for certain initial conditions it is possible that τ_{NL} is the only large non-linearity parameter, so the first observational signature of non-Gaussianity from this model could be the trispectrum through τ_{NL}.

Furthermore we have shown that during slow-roll inflation the loop corrections to the power spectrum, $f_{\rm NL}$ and τ_{NL} are always suppressed compared to the tree level terms. The suppression follows from the constraint on the background trajectory that the classical background value of the field should dominate over its quantum fluctuations.

We then investigated how the large non-Gaussianity which was generated during slow-roll may be changed by the effects from the end of inflation. We included the waterfall field which ends inflation when its effective mass becomes negative and it is destabilised. The effect of the waterfall field depends on the values of the coupling constants between the waterfall field and the two inflaton fields. If we choose the coupling constants so that surface where the waterfall field is destabilised corresponds to a hypersurface of uniform energy density then there is no change to the observables we calculated during slow roll. However if we choose the two coupling constants to be equal then observables at both linear and higher order are changed by an amount that depends on the ratio $\eta_{\varphi\varphi}/\eta_{\chi\chi}$.

Acknowledgments

The authors thank Yeinzon Rodriguez and Cesar Valenzuela-Toledo for numerous discussion on this work. CB thanks Martin Bucher, Paolo Creminelli, Daniel Figueroa, Sarah Shandera and is especially grateful to Bartjan van Tent, Misao Sasaki and Filippo Vernizzi for interesting discussions about this work. CB and K.-Y.C acknowledge STFC and the University of Sheffield for hospitality during a visit where part of this work was written. CB acknowledges financial support from the Deutsche Forschungsgemeinschaft. K.-Y.C. is supported by the Ministerio de Educacion y Ciencia of Spain under Proyecto Nacional FPA2006-05423 and by the Comunidad de Madrid under Proyecto HEPHACOS, Ayudas de I+D S-0505/ESP-0346. LMHH acknowledges support from STFC.

VI. APPENDIX

A. Loop Suppression

We require that the quantum fluctuation does not overwhelm the classical evolution of the fields. In order to do that we require $|\dot{\chi}|\pi/H^2 > \sqrt{3/2}$ for both fields on the background trajectory [47]. With this constraint we show that the tree level dominates the loop correction. In the slow-roll condition, this constraint leads to

$$|\varphi_*| > \sqrt{\frac{3}{2\pi^2}}\left|\frac{H_*}{\eta_{\varphi\varphi}}\right| \qquad \text{and} \quad |\chi_*| > \sqrt{\frac{3}{2\pi^2}}\left|\frac{H_*}{\eta_{\chi\chi}}\right|, \tag{48}$$

or equivelantly

$$\left|\frac{\delta\varphi_*}{\varphi_*}\right| < \left|\frac{\eta_{\varphi\varphi}}{\sqrt{6}}\right|, \qquad \left|\frac{\delta\chi_*}{\chi_*}\right| < \left|\frac{\eta_{\chi\chi}}{\sqrt{6}}\right|. \tag{49}$$

Using the δN formalism,

$$\delta N = N_\varphi\delta\varphi_* + N_\chi\delta\chi_* + \frac{1}{2}N_{\varphi\varphi}(\delta\varphi_*)^2 + \frac{1}{2}N_{\chi\chi}(\delta\chi_*)^2 + N_{\varphi\chi}(\delta\varphi_*)(\delta\chi_*) + \cdots, \tag{50}$$

in hybrid inflation, we find the first derivatives of the number of e-foldings

$$N_\varphi = \frac{\eta_{\varphi\varphi}\varphi_* e^{-2N\eta_{\varphi\varphi}}}{2\epsilon}, \qquad N_\chi = \frac{\eta_{\chi\chi}\chi_* e^{-2N\eta_{\chi\chi}}}{2\epsilon}, \tag{51}$$

and the second derivatives

$$\begin{aligned} N_{\varphi\varphi} &= \frac{N_\varphi}{\varphi_*} + \left(-4\eta_{\varphi\varphi} + 2\frac{\gamma}{\beta}\right)N_\varphi^2, \\ N_{\chi\chi} &= \frac{N_\chi}{\chi_*} + \left(-4\eta_{\chi\chi} + 2\frac{\gamma}{\beta}\right)N_\chi^2, \\ N_{\varphi\chi} &= 2N_\varphi N_\chi\left(\frac{\gamma}{\beta} - (\eta_{\varphi\varphi} + \eta_{\chi\chi})\right), \end{aligned} \tag{52}$$

where

$$\frac{\gamma}{\beta} = \frac{\eta_{\varphi\varphi}^3\varphi_*^2 e^{-2N\eta_{\varphi\varphi}} + \eta_{\chi\chi}^3\chi_*^2 e^{-2N\eta_{\chi\chi}}}{\eta_{\varphi\varphi}^2\varphi_*^2 e^{-2N\eta_{\varphi\varphi}} + \eta_{\chi\chi}^2\chi_*^2 e^{-2N\eta_{\chi\chi}}}. \tag{53}$$

We note that

$$\left|\frac{\gamma}{\beta}\right| < \eta_{max} \equiv \max\{\eta_{\varphi\varphi}, \eta_{\chi\chi}\}. \tag{54}$$

From the definition of the power spectrum and observations

$$\mathcal{P}_\zeta = \left(N_\varphi^2 + N_\chi^2\right)\left(\frac{H_*}{2\pi}\right)^2 \simeq 10^{-10}, \tag{55}$$

we know that

$$|N_\varphi \delta\varphi| \simeq |N_\varphi H_*| \lesssim 10^{-4}, \qquad |N_\chi \delta\chi| \simeq |N_\chi H_*| \lesssim 10^{-4}. \tag{56}$$

Using Eq. (49) and (56) we can easily check that the second order term in the expansion of δN are always smaller than the first order term. For example

$$\frac{1}{2}N_{\varphi\varphi}(\delta\varphi_*)^2 = \frac{1}{2}\frac{N_\varphi}{\varphi_*}(\delta\varphi_*)^2 + \left(-2\eta_\varphi + \frac{\gamma}{\beta}\right)(N_\varphi\delta\varphi_*)^2 < \frac{1}{2}\left(\frac{\eta_{\varphi\varphi}}{2\pi}\right)(N_\varphi\delta\varphi_*) + \eta_{max}10^{-5}(N_\varphi\delta\varphi_*) < |\eta_{\varphi\varphi}N_\varphi|\delta\varphi_*, \tag{57}$$

which is similar for the $N_{\chi\chi}$ term and

$$N_{\varphi\chi}(\delta\varphi_*\delta\chi_*) = 2(N_\varphi\delta\varphi_*)(N_\chi\delta\chi_*)\left(\frac{\gamma}{\beta} - (\eta_{\varphi\varphi} + \eta_{\chi\chi})\right) < 10^{-4}|\eta_{max}|\max(|N_\varphi|\delta\varphi_*, |N_\chi|\delta\chi_*). \tag{58}$$

The possible one loop domination can happen when χ is much smaller than $\delta\chi_*$, and $(\eta_{\varphi\varphi} - \eta_{\chi\chi})N > 1$ which is the case of Yeinzon et al. [22], but this can be possible only when we break the classical constraint we supposed in Eq. (49).

In [22, 23] the dominant loop correction to the power spectrum, bispectrum and trispectrum was found to come from a single loop diagram in each case which is the loop expansion one finds if truncating the δN expansion at second order. Specifically the loop corrections they found which may be dominant are (see figure 4)

$$\frac{P_\zeta^{1loop}}{P_\zeta^{tree}} = \frac{N_{AB}N_{AB}}{(N_C N_C)^2}\mathcal{P}_\zeta, \tag{59}$$

$$f_{NL}^{1\ \mathrm{loop}} = \frac{5}{6}\frac{N_{AB}N_{BC}N_{AC}}{(N_D N_D)^3}\mathcal{P}_\zeta, \tag{60}$$

$$\tau_{NL}^{1\,\mathrm{loop}} = \frac{N_{AB}N_{BC}N_{CD}N_{AD}}{(N_E N_E)^4}\mathcal{P}_\zeta. \tag{61}$$

Similar formula for f_{NL} and τ_{NL} at tree level are given in (19) (figure 3). By comparing the terms at tree and 1–loop level (which are suppressed by a factor of $\mathcal{P}_\zeta \sim 10^{-10}$) it is clear that the loop terms can only be large in the case that one of the second derivative terms in the δN expansion is extremely large. The integral over the loop momentum gives rise to a logarythmic infrared divergence $\ln(kL)$ where L is the large scale cut off. We have followed [22, 23, 46] in assuming that we can take $\ln(kL) \sim 1$. In the terminology of [54] this corresponds to working in a minimal box. For more discussion of this divergence see for example [45, 55, 56, 57].

Without loss of generality we assume $|N_{\varphi\varphi}| < \max(|\mathrm{N}_{\varphi\chi}|, |\mathrm{N}_{\chi\chi}|)$, so we need at least one of $|N_{\varphi\chi}|/N_\varphi^2 \gg 1$ or $|N_{\chi\chi}|/N_\varphi^2 \gg 1$ in order to have a significant loop correction. First we see that the cross derivative term is never large, using Eq. (51) and (52),

$$\frac{|N_{\varphi\chi}|}{N_\varphi^2 + N_\chi^2} < 4\frac{\sqrt{\tilde{r}}}{1+\tilde{r}}|\eta_{max}| < 2|\eta_{max}|. \tag{62}$$

The ratio which can be large is $N_{\chi\chi}/N_\varphi^2$, in the case that it is large we have the simplified formulas

$$\frac{P_\zeta^{1loop}}{P_\zeta^{tree}} \simeq \left(\frac{N_{\chi\chi}}{N_\varphi^2}\right)^2 \frac{1}{(1+\tilde{r})^2}\mathcal{P}_\zeta, \tag{63}$$

$$f_{NL}^{\rm tree} \simeq \frac{5}{6}\frac{N_{\chi\chi}}{N_\varphi^2}\frac{\tilde{r}}{(1+\tilde{r})^2}, \qquad f_{NL}^{1\ \rm loop} \simeq \frac{5}{6}\left(\frac{N_{\chi\chi}}{N_\varphi^2}\right)^3\frac{1}{(1+\tilde{r})^3}\mathcal{P}_\zeta, \tag{64}$$

$$\tau_{NL}^{\rm tree} \simeq \left(\frac{N_{\chi\chi}}{N_\varphi^2}\right)^2\frac{\tilde{r}}{(1+\tilde{r})^3}, \qquad \tau_{NL}^{1\,\rm loop} \simeq \left(\frac{N_{\chi\chi}}{N_\varphi^2}\right)^4\frac{1}{(1+\tilde{r})^4}\mathcal{P}_\zeta. \tag{65}$$

We recall the definition $\tilde{r} \equiv (N_\chi/N_\varphi)^2$. So it appears that by making $N_{\chi\chi}/N_\varphi^2$ large enough we can make the loop corrections as large as we like.

However using Eq. (56) and (57), we find the inequality

$$\left(\frac{N_{\chi\chi}}{N_\varphi^2}\right)^2\frac{\mathcal{P}_\zeta}{\tilde{r}(1+\tilde{r})} < \eta_{\chi\chi}^2 \ll 1, \tag{66}$$

and hence we see from (63) (64) and (65) that the loop correction to the power spectrum, $f_{\rm NL}$ and τ_{NL} is always suppressed.

B. Other loop corrections

So far we have proved that the loop corrections which [22, 23] found to be largest are still suppressed compared to the tree level terms. Here we show that these particular loop corrections remain the dominant loop corrections even for a more general trajectory in field space. To do this we need to go beyond second order in the δN expansion. In fact to prove that all of the 1–loop corrections to the power spectrum, $f_{\rm NL}$ and τ_{NL} are suppressed we need to go up to fourth order in the δN expansion.

At third order, the only derivatives which can be very large are

$$\frac{N_{\varphi\chi\chi}}{N_\varphi^3} = -2\eta_{\chi\chi}\frac{N_{\chi\chi}}{N_\varphi^2}, \qquad \frac{N_{\chi\chi\chi}}{N_\varphi^3} = 6\sqrt{\tilde{r}}(\eta_{\varphi\varphi}-2\eta_{\chi\chi})\frac{N_{\chi\chi}}{N_\varphi^2}, \tag{67}$$

while at fourth order the largest derivative is given by

$$\frac{N_{\chi\chi\chi\chi}}{N_\varphi^4} = 6(\eta_{\varphi\varphi}-2\eta_{\chi\chi})\left(\frac{N_{\chi\chi}}{N_\varphi^2}\right)^2. \tag{68}$$

We use the third order derivatives to calculate g_{NL}, see (19) and (21).

For details of the loop corrections we refer the reader to [45], in which a diaggrammatic approach to calculating the primordial n–point functions of ζ at any required loop level was developed. The formula for the n–point functions depend on the derivatives in the δN formalism, for every vertex with r internal legs there is a corresponding term with r derivatives of N. We note from Fig. 3 that the tree level diagrams for the power spectrum, $f_{\rm NL}$ and τ_{NL} all depend on diagrams with vertices connected to either one or two internal lines. The dominant loop correction found by [22, 23] in each case follows by adding an internal line between the two vertices with a single internal line attached in the tree level diagrams. These diagrams are shown in Fig. 4. This converts two first order derivatives of N into second order derivatives, which adds a large multiplicative factor of $(N_{\chi\chi}/N_\varphi^2)^2$ to the 1–loop term. When constructing any other 1–loop diagram we can either dress a vertex, which means adding two internal lines to a single vertex or connect an internal line between two external vertices where at least one of them does not have a single internal line atteched at tree level. In each of these cases it follows from (67) and (68) that these other diagrams are not boosted by a factor larger than $N_{\chi\chi}/N_\varphi^2$ and hence are subdominant to the loops found in [22, 23].

We conclude that all one-loop terms to the power spectrum, $f_{\rm NL}$ and τ_{NL} are suppressed compared to the tree level terms, even for a general trajectory in field space. In fact this argument applies to any loop term, provided that we can truncate the expansion of δN at fourth order. When drawing an $l+1$–loop level diagram we add an extra internal line to a diagram at l–loop level. This means attaching in total two extra derivatives to the derivatives of N corresponding to the vertices where the extra internal line is added. At most this can add a numerical factor of $(N_{\chi\chi}/N_\varphi^2)^2$. However there is also a suppression factor of order $\mathcal{P}_\zeta$ which comes from going to a higher order in loops, which as we have seen explicitly in the case of the one loops diagrams always leads to a suppression.

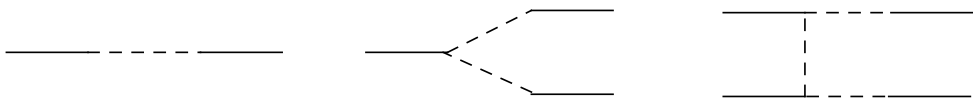

FIG. 3: Tree level diagrams for the power spectrum (left hand side), the bispectrum (centre) and the relevant tree diagram for the trispectrum (right) which corresponds to τ_{NL}. The diagrams were drawn using JAXODRAW [58]

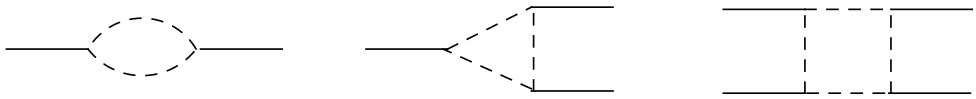

FIG. 4: The dominant one-loop level diagrams for the power spectrum (left hand side), the bispectrum (centre) and the trispectrum (right).

[1] E. Komatsu *et al.* [WMAP Collaboration], arXiv:0803.0547 [astro-ph].
[2] A. R. Liddle and D. H. Lyth, *Cambridge, UK: Univ. Pr. (2000) 400 p*
[3] N. Bartolo, E. Komatsu, S. Matarrese and A. Riotto, Phys. Rept. **402** (2004) 103 [arXiv:astro-ph/0406398].
[4] N. Bartolo, S. Matarrese and A. Riotto, Phys. Rev. D **65** (2002) 103505 [arXiv:hep-ph/0112261].
[5] L. Alabidi, JCAP **0610** (2006) 015 [arXiv:astro-ph/0604611].
[6] K. Enqvist, A. Jokinen, A. Mazumdar, T. Multamaki and A. Vaihkonen, Phys. Rev. Lett. **94** (2005) 161301 [arXiv:astro-ph/0411394].
[7] N. Barnaby and J. M. Cline, Phys. Rev. D **75**, 086004 (2007) [arXiv:astro-ph/0611750]; N. Barnaby and J. M. Cline, Phys. Rev. D **73**, 106012 (2006) [arXiv:astro-ph/0601481].
[8] B. Dutta, L. Leblond and J. Kumar, arXiv:0805.1229 [hep-th].
[9] A. Misra and P. Shukla, arXiv:0807.0996 [hep-th].
[10] E. Silverstein and D. Tong, Phys. Rev. D **70**, 103505 (2004) [arXiv:hep-th/0310221]; M. Alishahiha, E. Silverstein and D. Tong, Phys. Rev. D **70**, 123505 (2004) [arXiv:hep-th/0404084]; X. Chen, M. X. Huang, S. Kachru and G. Shiu, arXiv:hep-th/0605045; M. x. Huang and G. Shiu, Phys. Rev. D **74**, 121301 (2006) [arXiv:hep-th/0610235]; D. Langlois, S. Renaux-Petel, D. A. Steer and T. Tanaka, arXiv:0806.0336 [hep-th]; F. Arroja, S. Mizuno and K. Koyama, JCAP **0808**, 015 (2008) [arXiv:0806.0619 [astro-ph]].
[11] J. M. Maldacena, JHEP **0305**, 013 (2003) [arXiv:astro-ph/0210603].
[12] D. Seery and J. E. Lidsey, JCAP **0509**, 011 (2005) [arXiv:astro-ph/0506056].
[13] X. Chen, R. Easther and E. A. Lim, JCAP **0706**, 023 (2007) [arXiv:astro-ph/0611645].
[14] S. Mollerach, Phys. Rev. D **42** (1990) 313; A. D. Linde and V. F. Mukhanov, Phys. Rev. D **56**, 535 (1997) [arXiv:astro-ph/9610219]; K. Enqvist and M. S. Sloth, Nucl. Phys. B **626**, 395 (2002) [arXiv:hep-ph/0109214]; D. H. Lyth and D. Wands, Phys. Lett. B **524**, 5 (2002) [arXiv:hep-ph/0110002]; T. Moroi and T. Takahashi, Phys. Lett. B **522**, 215 (2001) [Erratum-ibid. B **539**, 303 (2002)] [arXiv:hep-ph/0110096]; K. Enqvist and S. Nurmi, JCAP **0510**, 013 (2005) [arXiv:astro-ph/0508573]; A. Linde and V. Mukhanov, JCAP **0604**, 009 (2006) [arXiv:astro-ph/0511736]; K. A. Malik and D. H. Lyth, JCAP **0609**, 008 (2006) [arXiv:astro-ph/0604387]; M. Sasaki, J. Valiviita and D. Wands, Phys. Rev. D **74**, 103003 (2006) [arXiv:astro-ph/0607627].
[15] L. Kofman, arXiv:astro-ph/0303614; G. Dvali, A. Gruzinov and M. Zaldarriaga, Phys. Rev. D **69**, 023505 (2004) [arXiv:astro-ph/0303591]; K. Ichikawa, T. Suyama, T. Takahashi and M. Yamaguchi, Phys. Rev. D **78**, 063545 (2008) [arXiv:0807.3988 [astro-ph]]; C. T. Byrnes, arXiv:0810.3913 [astro-ph].
[16] T. Suyama and M. Yamaguchi, Phys. Rev. D **77**, 023505 (2008) [arXiv:0709.2545 [astro-ph]].
[17] F. Bernardeau and J. P. Uzan, Phys. Rev. D **66** (2002) 103506 [arXiv:hep-ph/0207295]; F. Bernardeau and J. P. Uzan, Phys. Rev. D **67**, 121301 (2003) [arXiv:astro-ph/0209330]; F. Bernardeau and T. Brunier, Phys. Rev. D **76** (2007) 043526 [arXiv:0705.2501 [hep-ph]].
[18] D. H. Lyth, JCAP **0511**, 006 (2005) [arXiv:astro-ph/0510443]; M. P. Salem, Phys. Rev. D **72**, 123516 (2005) [arXiv:astro-ph/0511146].
[19] L. Alabidi and D. Lyth, JCAP **0608**, 006 (2006) [arXiv:astro-ph/0604569].
[20] M. Sasaki, Prog. Theor. Phys. **120**, 159 (2008) [arXiv:0805.0974 [astro-ph]].
[21] A. Naruko and M. Sasaki, Prog. Theor. Phys. **121**, 193 (2009) [arXiv:0807.0180 [astro-ph]].
[22] H. R. S. Cogollo, Y. Rodriguez and C. A. Valenzuela-Toledo, arXiv:0806.1546 [astro-ph].
[23] Y. Rodriguez and C. A. Valenzuela-Toledo, arXiv:0811.4092 [astro-ph].
[24] F. Vernizzi and D. Wands, JCAP **0605**, 019 (2006) [arXiv:astro-ph/0603799].
[25] K. Y. Choi, L. M. H. Hall and C. van de Bruck, JCAP **0702** (2007) 029 [arXiv:astro-ph/0701247].
[26] T. Battefeld and R. Easther, JCAP **0703**, 020 (2007) [arXiv:astro-ph/0610296].
[27] D. Seery and J. E. Lidsey, JCAP **0701**, 008 (2007) [arXiv:astro-ph/0611034].

[28] G. I. Rigopoulos, E. P. S. Shellard and B. J. W. van Tent, Phys. Rev. D **76**, 083512 (2007) [arXiv:astro-ph/0511041].
[29] S. Yokoyama, T. Suyama and T. Tanaka, Phys. Rev. D **77**, 083511 (2008) [arXiv:0705.3178 [astro-ph]]; S. Yokoyama, T. Suyama and T. Tanaka, arXiv:0711.2920 [astro-ph].
[30] C. T. Byrnes, K. Y. Choi and L. M. H. Hall, JCAP **0810** (2008) 008 [arXiv:0807.1101 [astro-ph]].
[31] A. A. Starobinsky, JETP Lett. **42**, 152 (1985) [Pisma Zh. Eksp. Teor. Fiz. **42**, 124 (1985)].
[32] M. Sasaki and E. D. Stewart, Prog. Theor. Phys. **95** (1996) 71 [arXiv:astro-ph/9507001].
[33] M. Sasaki and T. Tanaka, Prog. Theor. Phys. **99**, 763 (1998) [arXiv:gr-qc/9801017].
[34] D. H. Lyth, K. A. Malik and M. Sasaki, JCAP **0505**, 004 (2005) [arXiv:astro-ph/0411220].
[35] D. H. Lyth and Y. Rodriguez, Phys. Rev. Lett. **95** (2005) 121302 [arXiv:astro-ph/0504045].
[36] J. Garcia-Bellido and D. Wands, Phys. Rev. D **53** (1996) 5437 [arXiv:astro-ph/9511029].
[37] C. T. Byrnes, M. Sasaki and D. Wands, Phys. Rev. D **74**, 123519 (2006) [arXiv:astro-ph/0611075].
[38] N. Kogo and E. Komatsu, Phys. Rev. D **73**, 083007 (2006) [arXiv:astro-ph/0602099].
[39] K. Ichikawa, T. Suyama, T. Takahashi and M. Yamaguchi, Phys. Rev. D **78** (2008) 063545 [arXiv:0807.3988 [astro-ph]].
[40] K. Enqvist and S. Nurmi, JCAP **0510**, 013 (2005) [arXiv:astro-ph/0508573].
[41] Q. G. Huang and Y. Wang, JCAP **0809**, 025 (2008) [arXiv:0808.1168 [hep-th]].
[42] Q. G. Huang, JCAP **0811**, 005 (2008) [arXiv:0808.1793 [hep-th]].
[43] K. Enqvist and T. Takahashi, JCAP **0809**, 012 (2008) [arXiv:0807.3069 [astro-ph]].
[44] K. T. Engel, K. S. M. Lee and M. B. Wise, arXiv:0811.3964 [hep-ph].
[45] C. T. Byrnes, K. Koyama, M. Sasaki and D. Wands, JCAP **0711**, 027 (2007) [arXiv:0705.4096 [hep-th]].
[46] L. Boubekeur and D. H. Lyth, Phys. Rev. D **73**, 021301 (2006) [arXiv:astro-ph/0504046].
[47] P. Creminelli, S. Dubovsky, A. Nicolis, L. Senatore and M. Zaldarriaga, arXiv:0802.1067 [hep-th].
[48] D. H. Lyth and D. Wands, Phys. Rev. D **68** (2003) 103515 [arXiv:astro-ph/0306498].
[49] B. A. Bassett, S. Tsujikawa and D. Wands, Rev. Mod. Phys. **78**, 537 (2006) [arXiv:astro-ph/0507632].
[50] J. Garcia-Bellido and A. D. Linde, Phys. Rev. D **57**, 6075 (1998) [arXiv:hep-ph/9711360].
[51] X. Chen, Phys. Rev. D **72** (2005) 123518 [arXiv:astro-ph/0507053].
[52] M. LoVerde, A. Miller, S. Shandera and L. Verde, JCAP **0804**, 014 (2008) [arXiv:0711.4126 [astro-ph]].
[53] C. Rath, P. Schuecker and A. J. Banday, arXiv:astro-ph/0702163.
[54] D. H. Lyth, JCAP **0712**, 016 (2007) [arXiv:0707.0361 [astro-ph]].
[55] D. Seery, JCAP **0802**, 006 (2008) [arXiv:0707.3378 [astro-ph]].
[56] N. Bartolo, S. Matarrese, M. Pietroni, A. Riotto and D. Seery, JCAP **0801**, 015 (2008) [arXiv:0711.4263 [astro-ph]].
[57] K. Enqvist, S. Nurmi, D. Podolsky and G. I. Rigopoulos, JCAP **0804**, 025 (2008) [arXiv:0802.0395 [astro-ph]].
[58] D. Binosi and L. Theussl, Comput. Phys. Commun. **161**, 76 (2004) [arXiv:hep-ph/0309015].